Low Loss Electro-Optic Polymer Based Fast Adaptive Phase Shifters Realized in Silicon Nitride and Oxynitride Waveguide Technology

Lars Baudzus * and Peter M. Krummrich

Chair for High Frequency Technology, TU Dortmund, Friedrich-Woehler-Weg 4, Dortmund 44227, Germany; peter.krummrich@tu-dortmund.de
* Correspondence: lars.baudzus@tu-dortmund.de; Tel.: +49-231-755-4411

Abstract: We present a comprehensive study on how to design and fabricate low loss electro-optic phase shifters based on an electro-optic polymer and the silicon nitride and silicon oxynitride waveguide material systems. The loss mechanisms of phase shifters with an electro-optic (EO) polymer cladding are analyzed in detail and design solutions to achieve lowest losses are presented. In order to verify the low loss design a proof of concept prototype phase shifter was fabricated, which exhibits an attenuation of 0.8 dB/cm at 1550 nm and an electro-optic efficiency factor of 27%. Furthermore, the potential of this class of phase shifters is evaluated in numerical simulations, from which the optimal design parameters and achievable figures of merit were derived. The presented phase shifter design has its potential for application in fast adaptive multi stage devices for optical signal processing.

Keywords: integrated optics; phase shifter; phase modulator; silicon oxynitride; silicon nitride; electro-optic polymer

1. Introduction

Equalization enhances the robustness of data transmissions at high data rates in optical communication systems. It can be performed by digital signal processing, but also by optical signal processing [1,2]. The latter approach can save energy and costs and enables the implementation of functions, which are currently not realizable by digital signal processing. An optical equalizer can be implemented as an integrated optical filter, whose properties are adaptable by optical phase shifters. These kind of equalizers must have the ability to follow changes of the polarization dependent distortions, which can be on the timescale of µs [3,4]. Furthermore, a low optical attenuation is important to prevent excessive losses due to multiple stages in an optical equalizer. These requirements can be met by phase shifters based on the electro-optic (EO) effect. Phase shifters based on the thermo-optic effect are less power efficient and liquid crystals have typically a response time, which is too slow for their application in optical equalizers with real-time control.

The EO effect appears in different organic and inorganic materials. The most widespread EO material used in components for optical transmission systems is the inorganic crystal $LiNbO_3$. Furthermore, much effort has been devoted to the development of organic EO materials, which exhibit low optical losses and exceptionally high EO coefficients. At the current state of research, EO polymers [5] are the most convenient organic EO materials. They have advantages over organic EO crystals [6] and EO chromophore glasses [7], when thermal and long term stability, simplicity of processing and EO activity are considered.

Optical devices, which rely on EO polymers, can be separated into two designs. In one design an EO polymer is used as the waveguide core material. In this case an optical cladding material

is necessary, which has to posses not only a lower refractive index than the EO polymer but also a higher electrical conductivity. Otherwise, it is not possible to pole the EO polymer with a strong electrical field in order to activate its EO activity. Suitable cladding materials are certain epoxies [8] , DNA-CTMA [9] and sol-gel silica [10]. In the other design the EO polymer is used as the waveguide cladding material. Thereby, inorganic waveguide and electrode structures are fabricated typically by cost efficient complementary metal-oxide-semiconductor (CMOS) processes and the EO polymer cladding is added in a final step. Highly efficient EO modulators based on photonic-crystal [11], plasmonic [12] or slot waveguides [7] have been realized. Besides these devices, phase shifters can also be fabricated with a more simple fabrication process in the so-called "straightforward design". Thereby a rectangular waveguide core made from materials like silicon [13] or TiO_2 [14] is realized with a lateral electrode configuration as shown in Figure 1.
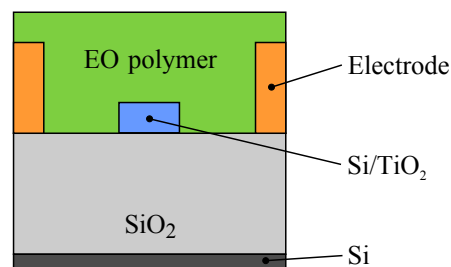
Figure 1. Straightforward design of an electro-optic (EO) polymer based phase shifter, where the EO polymer is used as cladding material.

The outstanding feature of silicon oxynitride (SiON) and silicon nitride (SiN) based planar optical waveguides is its ultra low loss. Planar waveguides with attenuations of under 0.1 dB/m have been realized [15]. First studies on the combination of the SiN waveguide technology and EO polymers have been successfully carried out [16,17]. The figure of merit (FOM) $V_\pi \cdot L$, which characterizes the necessary voltage V_π for a phase shift of π at a given electrode length L, was measured to 3.4 V·cm. However, the optical attenuations of the presented devices were over 10 dB/cm. These high values can be attributed to a non optimized design and fabrication process. The aim of this study is the elaboration of this optimization in order to demonstrate, that phase shifters based on SiON and SiN can also have a low attenuation. This makes them especially suitable for fast multistage optical signal processing devices.

In the following section the loss mechanisms in phase shifters based on SiON/SiN and an EO polymer in a straightforward design are analyzed in detail. Solutions to reduce the impacts of every loss mechanism are presented. In the third section the fabrication process and the measured properties of a prototype device are described, in order to verify the low loss design. The fourth section deals with the optimization of the design parameters by numerical simulations and the achievable figures of merit of this class of phase shifters. In a conclusion, the results are summarized and the relevance of this study is pointed out.

2. Design Solutions for Minimal Losses in SiON/SiN—EO Polymer Phase Shifters

2.1. Material Absorption

The vibrational modes of chemical bonds can be excited by the absorption of photons. This can occur, when the frequency of a photon is in the range of the frequency of the vibrational mode or an overtone. Absorptions at overtones of hydrogen bonds are relevant in the optical C-band, which is commonly used in optical communication systems.

SiON and SiN layers for waveguide applications are typically produced by plama-enhanced chemical vapor deposition (PECVD) or low-pressure chemical vapor deposition (LPCVD). They contain significant amounts of hydrogen due to the precursor gases. Si-H bonds absorb through the third

overtone around 1480 nm and N-H bonds absorb through the second overtone around 1510 nm. An annealing step at temperatures around 1150 °C can be performed after deposition in order to drive out the hydrogen [18].

However, the annealing step is problematic in two ways. On the one hand micromechanical or microelectronic systems cannot be integrated on the same chip before the annealing step. On the other hand SiON/SiN layers undergo high mechanical stress in the annealing process due to different thermal expansion coefficents than the silicon substrate. These highly stressed films tend to crack depending on their refractive index and film thickness. As shown in [18] SiON films with a refractive index up to 1.54 and in [19] up to 1.6 could be produced without cracks. These refractive indices are too low for EO polymer cladding designs, since EO polymers have typically higher refractive indices. In our study we were able to produce SiON waveguides with an arbitrary refractive index between 1.45 and 1.99 at 1550 nm by annealing the waveguide after etching it. Thereby the waveguide has to be etched to the underlying layer, so that no slab of the core material remains. Even at high indices and high waveguide heights no cracks or deformations could be observed. However, this approach can lead to stress induced birefringence of the waveguides. This drawback is not a problem with EO polymer phase shifters, because just one polarization mode is used anyway. Another approach is the use of deuterated precursor gases [20]. The deuteration shifts the absorptions to higher wavelengths with a sufficient distance to the C-band. A high temperature annealing would not be necessary, which enables a more convenient monolithic integration.

EO polymers typically consist of an optical polymer like poly(methyl methacrylate) (PMMA) or polycarbonate and an EO chromophore. They can be in a guest-host system or covalently joined. Especially the hydrogen bonds of these molecules can absorb light in the C-band. Unlike in the SiON/SiN layers the hydrogen cannot be removed or exchanged without drastically changing the properties of these materials. This means, that the absorption losses can only be reduced by improving the design of the chemical structure. Recently, a chromophore glass with an optical attenuation of 0.2 dB/cm has been demonstrated [7]. EO polymers usually show an attenuation of over 1 dB/cm [21].

2.2. Scattering Losses

Losses in an optical waveguide can be caused by scattering at rough edges. Whereas roughness at the surfaces of waveguides is rarely a problem and can be removed by chemical mechanical polishing (CMP), sidewall roughness can be a major source of attenuation [22]. Sidewall roughness can have its origin in lithography in the form of line edge roughness or in the plasma etching process. Optimized etching processes can result in a root mean square (RMS) roughnes of under 10 nm [23]. Besides the RMS roughness, the scattering losses depend on the power density of the mode fields at the sidewalls and the refractive indices of the core and cladding materials. Because of this, silicon waveguides have typically an attenuation, which is more than one order of magnitude higher than SiON or SiN waveguides due to a significant higher refractive index contrast between the waveguide core and the cladding.

Scattering can also occur at interfaces between layers of different types of materials, when the adhesion is problematic. In [24] the adhesion between a EO polymer and the SiON was insufficient, whereas in our study an insufficient adhesion was not identified as a source of attenuation.

2.3. Poling Induced Losses

In order to activate the EO properties of EO polymers, they have to be poled with an electric field of about 100 V/μm near the glass transition temperature. Thereby chromophores align to the electric field lines and a non-centrosymmetric symmetry arises, which is necessary for $\chi^{(2)}$ effects. In different studies a rise in optical attenuation was observed after poling [25,26]. This phenomenon can be explained by the formation of scattering centers during poling. Scattering centers can emerge from current or field induced damage in form of treeing or mechanical deformations, and from an inhomogeneous poling field distribution due to space charge regions or the waveguide design itself.

In order to reduce poling induced losses, space charge regions have to be prevented and the waveguide design has to be optimized for a homogenous poling field. It could be shown that a thin barrier layer between the electrode and the EO polymer can improve the poling process by reducing the leakage current and space charge induced inhomogeneities [27]. In EO polymer cladding phase shifters the waveguide core is located between two electrodes. Because of the different electric properties of the waveguide core material and the EO polymer, the electric field around the waveguide core becomes inhomogeneous [13]. Local maxima and minima in the electric potential emerge. This can lead to microphase separations in the EO polymer and consequently to scattering losses at these domains due to a local change in the refractive index. In this case scattering losses up to 10 dB per phase shifter were estimated in [13]. To overcome this problem, we propose the deposition of an additional SiO_2 or SiON layer over the waveguide core and a subsequent planarization by CMP. The change in the design, which leads to a more homogenous poling field, is illustrated in Figure 2.
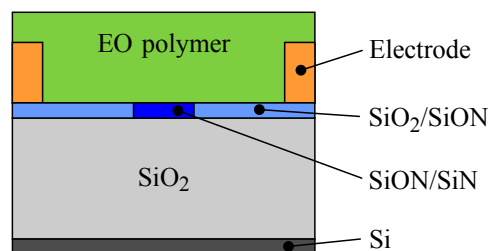
Figure 2. Optimized waveguide design, which enables a more homogenous poling field to reduce poling induced losses.

Another poling related loss mechanism is the attenuation at interfaces from poled to non-poled areas and vice versa. This attenuation is caused by the mismatch of the mode fields in each area due to the change of the refractive index during poling. A birefringence of over 0.05 can be induced in this process. Although the attenuation at these transitions is small compared to other mechanisms, it is reasonable to be taken into account in multistage devices with a high number of optical phase shifters [1,2]. A solution to this problem is the introduction of a SiON cladding layer between the poled areas. Thereby the refractive index of the SiON is matched to the refractive index of the poled EO polymer, so that no transitions between areas with different mode fields arise. The SiON cladding layer can also be used as a bridge over the waveguide to connect electrodes with contact pads. These benefits are illustrated in Figure 3. In [17] SiO_2 was used as a bridge over the waveguide in a similar design. A transition loss of 0.5 dB per transition was estimated, due to the difference between the refractive indices of SiO_2 and the EO polymer. These losses are prevented in the proposed design.
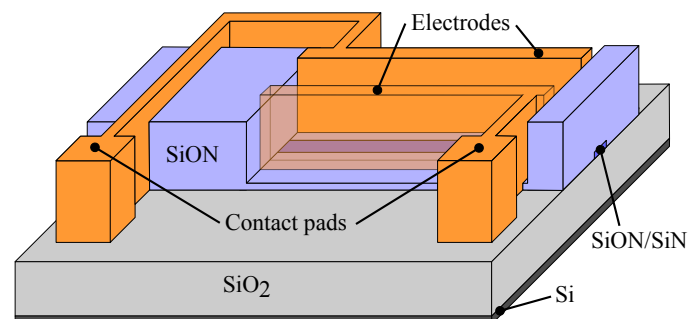
Figure 3. Refractive index matched SiON cladding, which reduces transition losses between poled and non-poled areas and can also be used as bridges over the waveguides in order to connect the electrodes with the contact pads.

2.4. Fiber-Chip Coupling Losses

The fiber to chip or respectively the chip to fiber coupling losses represent crucial contributions for the insertion loss of a device. The large mode field diameter (MFD) of a standard single mode fiber (SSMF) mode has to be converted to a typically smaller MFD of a planar optical waveguide mode. Different approaches exist for this problem. These include grating couplers [28], high numerical aperture fibers (HNAF) [18], lensed fibers [29], cantilever [30], and taper structures [31]. Whereas the coupling to typical SiON waveguides is unproblematic, because SSMFs [32] or HNAFs [18] can be directly butt coupled to the waveguides with losses around 0.35 dB, the coupling to higher refractive index contrast SiON or SiN waveguides is more challenging. However coupling losses under 1 dB were experimentally demonstrated [30,31]. Therefore, the coupling of light from a SSMF to a high index contrast SiON or SiN waveguide with low losses can be considered as being a solved problem.

3. Proof of concept Prototype

3.1. Fabrication Process

In order to verify the low loss design a prototype with a cross section according to Figure 2 was fabricated. In a first step we deposited 6 μm SiO_x and 0.8 μm SiON with a refractive index of 1.63 at 1550 nm by PECVD on a 4″ silicon wafer in an Oxford Plasmalab System 100. The gases SiH_4, Ar and N_2O were used for the SiO_x layer with gas flows of 5 sccm, 95 sccm and 500 sccm, respectively. For the SiON layer the gases SiH_4, Ar, NH_3, N_2O and N_2 were used with gas flows of 10 sccm, 180 sccm, 10 sccm, 60 sccm and 500 sccm, respectively. In both processes the pressure was 800 mTorr, the temperature 390 °C and the RF power 50 W. In the next step a photoresist etching mask for straight waveguides was patterned by broadband UV contact lithography. The photoresist pattern was etched in the SiON layer by reactive ion etching (RIE) in a Plasma Technology RIE System 80. The gases Ar, CHF_3 and O_2 were used with gas flows of 168 sccm, 40 sccm and 5 sccm, respectively. The pressure in the chamber was 80 mTorr and the self bias 150 V. A PECVD SiO_x layer was deposited afterwards and subsequently planarized by CMP. At the ends of the waveguides 4 μm PECVD SiO_x was deposited to reduce fiber to chip coupling losses. Afterwards the wafer was annealed at 1170 °C for 12 h in a N_2 atmosphere. Electrodes were added in a lift-off process, whereby 1.6 μm Cr/Cu was deposited by electron-beam evaporation. The wafer was cut in a way that samples with different length were formed and the facets of each sample were polished. Disperse Red 1 and PMMA were dissolved in Anisol with a mass fraction of 1% and 9%, respectively. The solution was drop casted onto the samples, which were subsequently cured for 12 h at 65 °C. The electrodes were contacted by micro needles and the EO polymer was poled at 95 °C and a voltage of 1 kV. A scanning electron microscope (SEM) picture of the active region of a prototype device before the EO polymer deposition is shown in Figure 4.
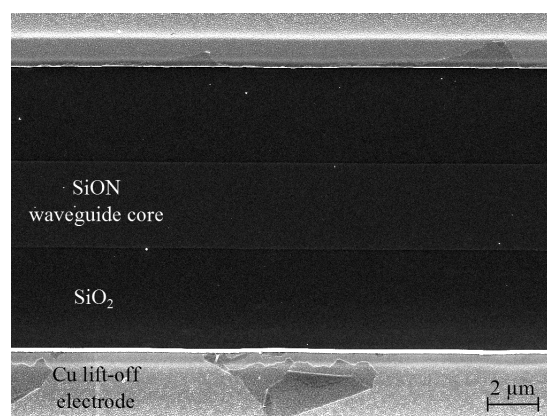

Figure 4. SEM picture of the active region of a fabricated prototype device.

The resulting prototype devices have a core width of 3.5 μm, a core height of 0.7 μm, a core refractive index of 1.64 and an electrode distance of 11 μm. For this parameters an EO efficiency factor η of 27% was calculated by numerical simulation. The EO efficiency factor is defined as $\eta = \Delta n_{\text{eff}}/\Delta n_{\text{EO polymer}}$. Here Δn_{eff} is the change in the effective index of the waveguide mode, when the refractive index of the EO polymer cladding is changed by $\Delta n_{\text{EO polymer}}$.

3.2. Measurement Procedure

In order to determine the optical attenuation of the prototype devices the optical losses of multiple phase shifters on each sample were measured. The samples were fixed on a vacuum sample holder and Nufern UHNA4 fibers attached to piezo actuators were positioned in front of the waveguide end facet of the phase shifter under test. A laser source emitting at 1550 nm and an optical power meter were used to measure the optical loss.

For the study of the EO-activity the set-up for the optical attenuation measurement was extended by a fiber based Mach-Zehnder interferometer (MZI) as shown in Figure 5. A prototype phase shifter was positioned in one arm of the MZI. The electrodes were contacted by micro needles and a modulation signal with a frequency of 1 kHz was applied. The output power of the MZI was analyzed by a photodiode and an oscilloscope.
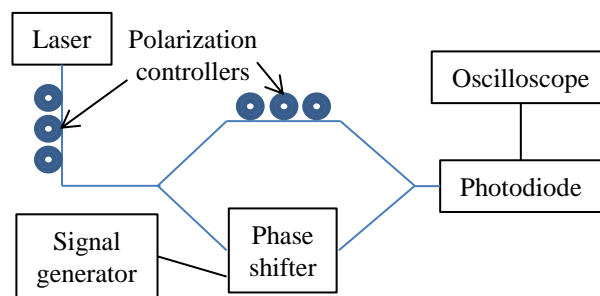

Figure 5. Diagram of the set-up for the study of the EO activity.

3.3. Measurement Results and Discussion

The attenuation was determined to 0.8 dB/cm. It was calculated from the losses of samples with different lengths in order to distinguish between the losses due to fiber chip coupling and waveguide attenuation. On each sample the losses for multiple waveguides with the same length were averaged and a measurement error of 0.1 dB/cm was determined. The measured attenuation is more than one order of magnitude smaller than in a previously reported phase shifter, which was fabricated from similar waveguide materials [17]. The attenuation can mainly be attributed to absorption and scattering in the EO polymer. Residues of the lift of process, which can be seen in Figure 4 as small white dots, can also contribute to the attenuation, when they are not fully removed in a cleaning process. Absorptions by SiON, SiO$_2$ and the copper electrodes have a minor influence on the attenuation, because hydrogen bonds were removed in the annealing process and the distance from the waveguide core to the electrodes is sufficiently high. Sidewall roughness was also identified as a minor source of attenuation, because an optimized RIE process was used. The resulting sidewall roughness of the etching process is illustrated in Figure 6, in which an etched waveguide without a cladding is shown.

From the analysis of the oscilloscope data the FOM $V_\pi \cdot L$ was estimated to be 900 V·cm. This high value can mainly be attributed to the relatively low EO coefficient of the EO polymer. PMMA/Disperse Red 1 thin films poled at fields around 100 V/μm exhibit a r_{33} value of about 3 pm/V [33], while thin films prepared with state-of-the-art EO polymers and poled at similar fields show r_{33} values of over 100 pm/V [5]. Furthermore, an optimized phase shifter design with a smaller electrode distance, can reduce the FOM by a factor of about 2.5. The optimization of the phase shifter design is elaborated in Section 4. A r_{33} value of 1.7 pm/V can be estimated for the EO polymer in the prototype device,

which is lower than the reference value of 3 pm/V. This indicates, that the poling process can be further optimized. The use of a state-of-the-art EO polymer, an optimized design and an optimized poling process can enable a reduction of $V_\pi \cdot L$ by about two orders of magnitude. The properties of a previously demonstrated phase shifter, which was fabricated from similar waveguide materials but with a state-of-the-art EO polymer, support this estimation [17].
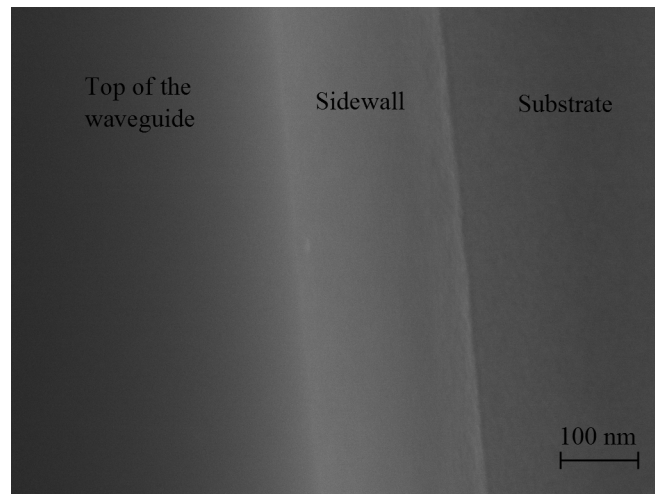
Figure 6. SEM picture, which illustrates the low sidewall roughness resulting from an optimized etching process.

4. Optimization of the Phase Shifter Design

4.1. Simulation Set-up

The loss per phase shifter was optimized by the variation of the refractive index profile in numerical simulations in order to evaluate the full potential of the phase shifter design. Whereas in most studies on EO modulators the FOM $V_\pi \cdot L$ is optimized, which can be interpreted as an optimization of the footprint of the device for a given voltage, we focus on the FOM $V_\pi \cdot L \cdot \alpha_{dB}$, which characterizes the losses per phase shifter for a given voltage. Here α_{dB} is the attenuation in the active region of the phase shifter. In our simulations we calculate the complex effective index for different design parameters and derive the FOMs from it. A semi vectorial finite difference beam propagation method is used to calculate the effective indices. In the analysis of our results we "normalize" the FOMs by multiplying them by the EO coefficient r_{33} in order to make the results valid for EO polymers with arbitrary EO coefficients. The result for a specific EO polymer can be obtained by dividing the "normalized" value by the r_{33} of this EO polymer.

In our simulations the design of Figure 2 was used. The side cladding was defined as SiON with a refractive index matching the one of the EO polymer. We set the attenuation coefficients to 0.05 dB/cm for SiON, 1 dB/cm for the EO polymer, and neglected the losses in SiO$_2$. The properties of copper were used for the simulated electrodes. The influences of sidewall roughness were neglected due to the relatively low refractive index contrast and the state-of-the-art etching processes.

In a first set of simulations the refractive index of the EO polymer was set to 1.62, which corresponds to a state-of-the-art low refractive index EO polymer [5], and the waveguide width was set to 3 μm. For different refractive indices of the core ranging from 1.75 to 1.99 the height and the electrode distance was varied to identify an optimal $V_\pi \cdot L \cdot \alpha_{dB} \cdot r_{33}$. The aim of this first set of simulations is to find the optimal refractive index contrast between the waveguide core and the EO polymer.

In a second set of simulations the refractive index of the core was set to 1.99 and the EO polymer to 1.7, which corresponds to a common refractive index of a state-of-the-art EO polymer [5]. The choice of parameters was influenced by the results of the first set of simulations. The core height, width and electrode distance were optimized.

In a third set of simulations the optimized height and the width of the second set of simulations were used. The attenuation of the EO polymer was varied from 0.5 dB/cm to 3 dB/cm and the electrode distance was optimized for each value. In this set of simulations the validity of the optimized parameters for EO polymers with an refractive index of 1.7 and arbitrary values of α_{dB} and r_{33} is analyzed.

4.2. Simulation Results and Discussion

The results of the first set of simulations are shown in Figure 7. It can be seen that the values of $V_\pi \cdot L \cdot \alpha_{dB} \cdot r_{33}$ and $V_\pi \cdot L \cdot r_{33}$ are getting lower with increasing core refractive index. The reason for this is a faster decay of the mode fields in the cladding at higher index contrasts, which enables a shorter electrode distance. The lowest value for $V_\pi \cdot L \cdot \alpha_{dB} \cdot r_{33}$ can be found at the highest core refractive index, which corresponds to SiN. At higher refractive indices of SiON, EO polymers with higher refractive indices can be used and are preferable because of their typically larger EO coefficient compared to lower refractive index materials.
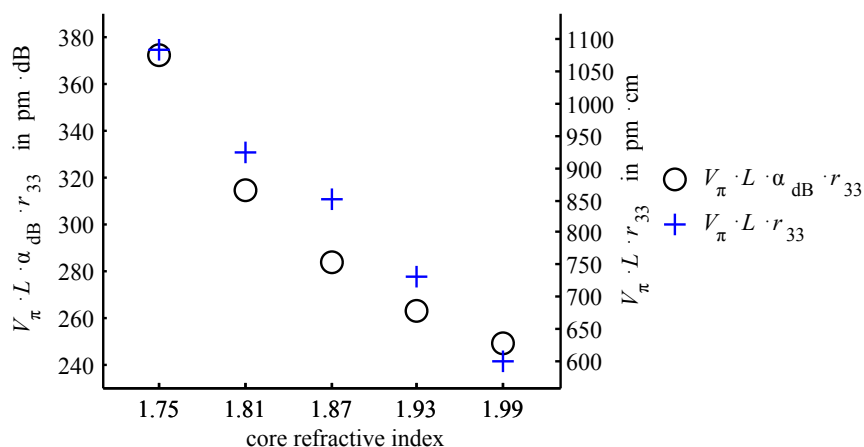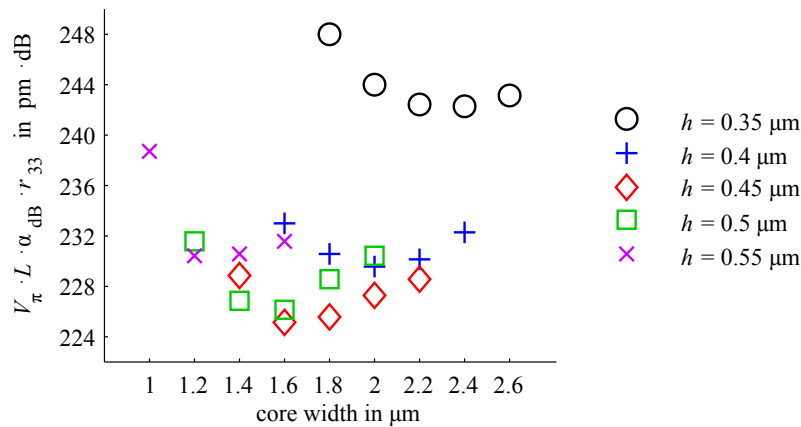

**Figure 7.** Results of the simulations to determine the optimal core refractive index.

The results of the second set of simulations are shown in Figure 8. For every waveguide height h one optimal width exists. Widths, which are too large or too small, extend the mode field in the horizontal direction. This increases the required electrode spacing. A similar behavior can be seen, when the height is changed. At smaller heights than the optimum the mode field is less confined in the waveguide core and expanded in the horizontal direction. The higher amount of field in the EO polymer does not lead to a better FOM, because the electrodes have to be placed disproportionally further apart. When the height is larger than the optimum, the mode field is more confined in the waveguide core and is more contracted in the horizontal direction, but the electrodes cannot be reduced proportionally to the lower amount of field in the EO polymer.

The results of the third set of simulations are shown in Figure 9. With increasing EO polymer attenuation $V_\pi \cdot L \cdot \alpha_{dB} \cdot r_{33}$ rises nearly linear. However a decreasing optimal electrode distance can cause a slight deviation from the linear case. This deviation is estimated to be neglectable, which indicates, that the optimal parameters are valid for every simulated EO polymer attenuation.

Figure 8. Results of the simulations to optimize the core dimensions at a core refractive index of 1.99 and an EO polymer refractive index of 1.7.
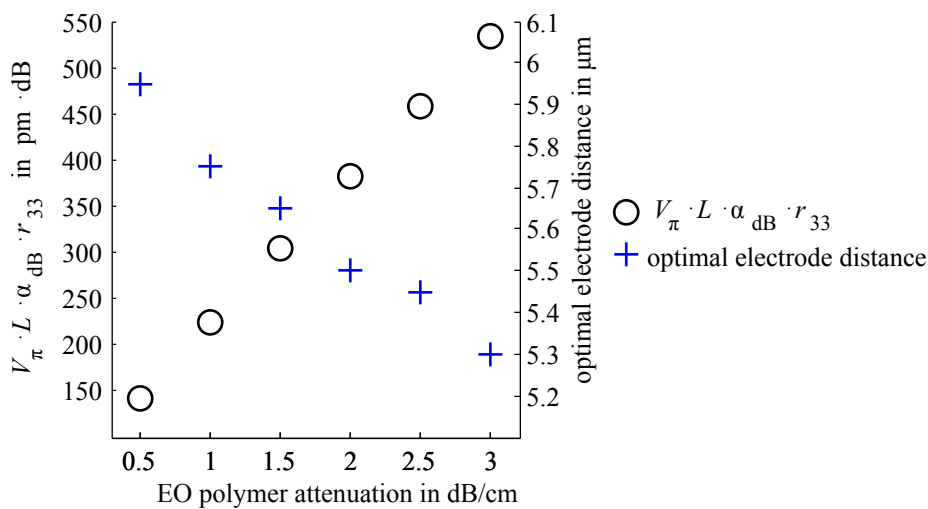
Figure 9. Simulation results, which show $V_\pi \cdot L \cdot \alpha_{dB} \cdot r_{33}$ and the optimal electrode distance in dependence of the EO polymer attenuation for the optimized waveguide dimensions.

In summary, optimal design parameters were derived, which are valid for EO polymers with a refractive index of 1.7, arbitrary r_{33} values and attenuations ranging from 0.5 db/cm to 3 db/cm. The optimal waveguide core refractive index is 1.99. A global minimum of $V_\pi \cdot L \cdot \alpha_{dB} \cdot r_{33}$ can be identified at 0.45 μm height and 1.6 μm width. The optimal electrode distance is between 5.3 μm and 6 μm depending on the EO polymer attenuation.

To the best of our knowledge the lowest value for $V_\pi \cdot L \cdot \alpha_{dB}$ for an EO polymer based phase shifter, which can be derived from reported results, is 2.86 V·dB in push pull configuration and 5.72 V·dB in single phase modulator operation [7]. This corresponds to a simulated phase shifter in our design, in which an EO polymer with an attenuation of 1 dB/cm and an r_{33} of about 39 pm/V is used. These values are feasible for an in-device EO polymer in a future phase shifter in the presented design. The simulation results indicate, that the proposed design is a serious candidate for an EO polymer based phase shifter with the lowest losses at a given driving voltage.

5. Conclusions

We have shown, that the SiON and SiN material systems can be combined with EO polymers to realize fast adaptive phase shifters with a very low attenuation. A proof of concept prototype exhibited an attenuation of 0.8 dB/cm at 1550 nm and an EO efficiency factor of 27%. This attenuation

is one order of magnitude lower than the attenuation in a device previously reported [17], which was fabricated from similar waveguide materials. In numerical simulations a set of design parameters could be determined, which optimizes the losses per phase shifter for a given driving voltage. This class of phase shifters can be produced by established cost efficient CMOS processes, which are already used for the production of SiON and SiN based passive optical components.

In future work the optimized fabrication process and design parameters from this study can be combined with a state-of-the-art EO polymer to realize phase shifters, which have the serious potential to possess lowest losses at a given driving voltage. Although the $V_\pi \cdot L$ of the presented phase shifter design is generally higher than in slot waveguide, plasmonic or photonic crystal based devices, which makes these designs preferable for optical modulators, the low optical attenuation in our design enables the application in adaptive multistage devices for powerful optical signal processing and equalization.

Abbreviations

The following abbreviations are used in this manuscript:

EO	electro-optic
CMOS	complementary metal-oxide-semiconductor
SiON	silicon oxynitride
SiN	silicon nitride
FOM	figure of merit
PECVD	plasma-enhanced chemical vapor deposition
LPCVD	low-pressure chemical vapor deposition
PMMA	poly(methyl methacrylate)
CMP	chemical mechanical polishing
RMS	root mean square
MFD	mode field diameter
SSMF	standard single mode fiber
HNAF	high numerical aperture fiber
MZI	Mach-Zehnder interferometer
RIE	reactive ion etching
SEM	scanning electron microscope

References

1. Bohn, M.; Rosenkranz, W.; Krummrich, P. Adaptive distortion compensation with integrated optical finite impulse response filters in high bitrate optical communication systems. *IEEE J. Sel. Top. Quantum Electron.* **2004**, *10*, 273–280.

2. Doerr, C.; Fontaine, N.; Buhl, L. PDM-DQPSK Silicon Receiver with Integrated Monitor and Minimum Number of Controls. *IEEE Photonics Technol. Lett.* **2012**, *24*, 697–699.

3. Krummrich, P.; Kotten, K. Extremely fast (microsecond timescale) polarization changes in high speed long haul WDM transmission systems. In Proceedings of the Optical Fiber Communication Conference, Los Angeles, CA, USA, 23–27 February 2014; Volume 2, p. 3.

4. Krummrich, P.M.; Ronnenberg, D.; Schairer, W.; Wienold, D.; Jenau, F.; Herrmann, M. Demanding response time requirements on coherent receivers due to fast polarization rotations caused by lightning events. *Opt. Express* **2016**, *24*, 12442–12457.

5. Luo, J.; Jen, A.Y. Highly Efficient Organic Electrooptic Materials and Their Hybrid Systems for Advanced Photonic Devices. *IEEE J. Sel. Top. Quantum Electron.* **2013**, *19*, 42–53.

6. Korn, D.; Jazbinsek, M.; Palmer, R.; Baier, M.; Alloatti, L.; Yu, H.; Bogaerts, W.; Lepage, G.; Verheyen, P.; Absil, P.; et al. Electro-Optic Organic Crystal Silicon High-Speed Modulator. *IEEE Photonics J.* **2014**, *6*, 1–9.

7. Palmer, R.; Koeber, S.; Elder, D.; Woessner, M.; Heni, W.; Korn, D.; Lauermann, M.; Bogaerts, W.; Dalton, L.; Freude, W.; et al. High-Speed, Low Drive-Voltage Silicon-Organic Hybrid Modulator Based on a Binary-Chromophore Electro-Optic Material. *J. Lightwave Technol.* **2014**, *32*, 2726–2734.

8. Kim, S.K.; Zhang, H.; Chang, D.; Zhang, C.; Wang, C.; Steier, W.; Fetterman, H. Electrooptic polymer modulators with an inverted-rib waveguide structure. *IEEE Photonics Technol. Lett.* **2003**, *15*, 218–220.

9. Heckman, E.M.; Aga, R.S.; Rossbach, A.T.; Telek, B.A.; Bartsch, C.M.; Grote, J.G. DNA biopolymer conductive cladding for polymer electro-optic waveguide modulators. *Appl. Phys. Lett.* **2011**, *98*, doi:10.1063/1.3562953.

10. DeRose, C.T.; Himmelhuber, R.; Mathine, D.; Norwood, R.A.; Luo, J.; Jen, A.K.Y.; Peyghambarian, N. High Δn strip-loaded electro-optic polymer waveguide modulator with low insertion loss. *Opt. Express* **2009**, *17*, 3316–3321.

11. Zhang, X.; Hosseini, A.; Lin, C.Y.; Luo, J.; Jen, A.Y.; Chen, R. Demonstration of effective in-device r33 over 1000 pm/V in electro-optic polymer refilled silicon slot photonic crystal waveguide modulator. In Proceedings of the Conference on Laser and Electro-Optics Event (CLEO), San Jose, CA, USA, 9–14 June 2013; pp. 1–2.

12. Melikyan, A.; Koehnle, K.; Lauermann, M.; Palmer, R.; Koeber, S.; Muehlbrandt, S.; Schindler, P.C.; Elder, D.L.; Wolf, S.; Heni, W.; et al. Plasmonic-organic hybrid (POH) modulators for OOK and BPSK signaling at 40 Gbit/s. *Opt. Express* **2015**, *23*, 9938–9946.

13. Himmelhuber, R.; Herrera, O.; Voorakaranam, R.; Li, L.; Jones, A.; Norwood, R.; Luo, J.; Jen, A.Y.; Peyghambarian, N. A Silicon-Polymer Hybrid Modulator —Design, Simulation and Proof of Principle. *J. Lightwave Technol.* **2013**, *31*, 4067–4072.

14. Qiu, F.; Spring, A.M.; Maeda, D.; Ozawa, M.a.; Odoi, K.; Aoki, I.; Otomo, A.; Yokoyama, S. A straightforward electro-optic polymer covered titanium dioxide strip line modulator with a low driving voltage. *Appl. Phys. Lett.* **2014**, *105*, doi:10.1063/1.4893925.

15. Bauters, J.F.; Heck, M.J.R.; John, D.D.; Barton, J.S.; Bruinink, C.M.; Leinse, A.; Heideman, R.G.; Blumenthal, D.J.; Bowers, J.E. Planar waveguides with less than 0.1 dB/m propagation loss fabricated with wafer bonding. *Opt. Express* **2011**, *19*, 24090–24101.

16. Block, B.A.; Younkin, T.R.; Davids, P.S.; Reshotko, M.R.; Chang, P.; Polishak, B.M.; Huang, S.; Luo, J.; Jen, A.K.Y. Electro-optic polymer cladding ring resonator modulators. *Opt. Express* **2008**, *16*, 18326–18333.

17. Block, B.; Liff, S.; Kobrinsky, M.; Reshotko, M.; Tseng, R.; Ban, I.; Chang, P. A low power electro-optic polymer clad Mach-Zehnder modulator for high speed optical interconnects. *Proc. SPIE Silicon Photonics* **2013**, *8629*, doi:10.1117/12.2004489.

18. Fadel, M.; Bulters, M.; Niemand, M.; Voges, E.; Krummrich, P. Low-Loss and Low-Birefringence High-Contrast Silicon-Oxynitride Waveguides for Optical Communication. *J. Lightwave Technol.* **2009**, *27*, 698–705.

19. Albers, H.; Hilderink, L.; Szilagyi, E.; Paszti, F.; Lambeck, P.; Popma, T. Reduction of hydrogen induced losses in PECVD-SiO$_x$N$_y$ optical waveguides in the near infrared. In Proceedings of the 8th Annual Meeting Conference on Lasers and Electro-Optics Society Annual Meeting, San Francisco, CA, USA, 30 October–2 November 1995; pp. 88–89.

20. Johnson, F.G.; King, O.S.; Hryniewicz, J.V.; Joneckis, L.G.; Chu, S.T.; Gill, D.M. Use of Deuterated Gases for the Vapor Deposition of Thin Films for Low-Loss Optical Devices and Waveguides. U.S. Patent 6,771,868 B2, 2004.

21. DeRose, C. *Electro-Optic Polymers: Materials and Devices*; University of Arizona: Tucson, AZ, USA, 2009.

22. Barwicz, T.; Haus, H. Three-dimensional analysis of scattering losses due to sidewall roughness in microphotonic waveguides. *J. Lightwave Technol.* **2005**, *23*, 2719–2732.

23. Jang, J.H.; Zhao, W.; Bae, J.W.; Selvanathan, D.; Rommel, S.L.; Adesida, I.; Lepore, A.; Kwakernaak, M.; Abeles, J.H. Direct measurement of nanoscale sidewall roughness of optical waveguides using an atomic force microscope. *Appl. Phys. Lett.* **2003**, *83*, 4116–4118.

24. De Ridder, R.M.; Driessen, A.; Rikkers, E.; Lambeck, P.V.; Diemeer, M.B. Design and fabrication of electro-optic polymer modulators and switches. *Opt. Mater.* **1999**, *12*, 205–214.

25. Teng, C.C.; Mortazavi, M.A.; Boudoughian, G.K. Origin of the poling-induced optical loss in a nonlinear optical polymeric waveguide. *Appl. Phys. Lett.* **1995**, *66*, 667–669.
26. Chen, H.; Chen, B.; Huang, D.; Jin, D.; Luo, J.D.; Jen, A.K.Y.; Dinu, R. Broadband electro-optic polymer modulators with high electro-optic activity and low poling induced optical loss. *Appl. Phys. Lett.* **2008**, *93*, doi:10.1063/1.2965809.
27. Huang, S.; Kim, T.D.; Luo, J.; Hau, S.K.; Shi, Z.; Zhou, X.H.; Yip, H.L.; Jen, A.K.Y. Highly efficient electro-optic polymers through improved poling using a thin TiO_2-modified transparent electrode. *Appl. Phys. Lett.* **2010**, *96*, doi:10.1063/1.3453659.
28. Taillaert, D.; Laere, F.V.; Ayre, M.; Bogaerts, W.; Thourhout, D.V.; Bienstman, P.; Baets, R. Grating Couplers for Coupling between Optical Fibers and Nanophotonic Waveguides. *Jpn. J. Appl. Phys.* **2006**, *45*, 6071.
29. Edwards, C.; Presby, H.M.; Dragone, C. Ideal microlenses for laser to fiber coupling. *J. Lightwave Technol.* **1993**, *11*, 252–257.
30. Chen, L.; Doerr, C.; Chen, Y.K.; Liow, T.Y. Low-Loss and Broadband Cantilever Couplers Between Standard Cleaved Fibers and High-Index-Contrast Si_3N_4 or Si Waveguides. *IEEE Photonics Technol. Lett.* **2010**, *22*, 1744–1746.
31. Shoji, T.; Tsuchizawa, T.; Watanabe, T.; Yamada, K.; Morita, H. Spot-size converter for low-loss coupling between 0.3 μm-square Si wire waveguides and single-mode fibers. In Proceedings of the 15th IEEE Annual Meeting of the Lasers and Electro-Optics Society, Glasgow, UK, 10–14 November 2002; pp. 289–290.
32. Hoffmann, M.; Kopka, P.; Voges, E. Low-loss fiber-matched low-temperature PECVD waveguides with small-core dimensions for optical communication systems. *IEEE Photonics Technol. Lett.* **1997**, *9*, 1238–1240.
33. Singer, K.D.; Holland, W.R.; Kuzyk, M.G.; Wolk, G.L.; Cahill, P.A. Guest-Host Polymers for Nonlinear Optics. *Mol. Cryst. Liq. Cryst. Inc. Nonlinear Opt.* **1990**, *189*, 123–136.